Journal of the Chinese Institute of Engineers, Vol. 22, No. 6, pp. 677-693 (1999)

A DISLOCATION AND POINT FORCE APPROACH TO THE BOUNDARY ELEMENT METHOD FOR MIXED MODE CRACK ANALYSIS OF PLANE ANISOTROPIC SOLIDS

Mitsunori Denda
Rutgers University
Mechanical and Aerospace Engineering Department
98 Brett Road, Piscataway, New Jersey 08854-8058, U.S.A.

Key Words: boundary element method, plane anisotropic elasticity, dislocation and point force approach, mixed mode crack analysis.

ABSTRACT

In this paper we formulate a direct boundary element method (BEM) for plane anisotropic elasticity (i.e., the in-plane deformation decoupled from the out-of-plane deformation) based on distributions of point forces and dislocation dipoles. According to a physical interpretation of Somigliana's identity the displacement field in a finite body R is represented by the continuous distributions of point forces and dislocation dipoles along the imaginary boundary ∂R of the finite domain R embedded in an infinite body. We adopt Stroh's complex variable formalism for anisotropic elasticity and represent the point force and the dislocation, their dipoles, and continuous distributions systematically exploiting the duality relations between the point force and the dislocation solutions. Explicit formulas for the displacement and the traction formulations, obtained by analytical integration of the boundary integrals, are given. We apply these formulas to mixed mode crack problems for multiply cracked anisotropic bodies by extending the physical interpretation of Somigliana's identity to cracked bodies and representing the crack by the continuous distribution of dislocation dipoles. With the help of the conservation integrals of anisotropic elasticity, we will demonstrate the capability of the method to determine the mixed mode stress intensity factors (K_I and K_{II}) accurately.

I. INTRODUCTION

The majority of the BEM formulations in two-dimensional anisotropic elasticity are based on the Somigliana's identity and its mathematical interpretation. This leads to the direct formulation (Rizzo and Shippy, 1970; Benjumea and Sikarskie, 1972; Balas *et al.*, 1989, Sollero and Aliabadi, 1993) in terms of the fundamental displacement and traction solutions for the point force in an infinite body. In this paper we adopt a physical (rather than mathematical) interpretation of Somigliana's identity to formulate the direct BEM in terms of the point force and the dislocation dipole solutions. Other seemingly different formulations in the indirect BEM, such as the method of the continuous distribution of body forces (Lee and Mal, 1990) and the continuous distribution of dislocations (Crouch and Starfield, 1983), can all be derived from this physical interpretation of Somigliana's identity as shown by Maiti *et al.* (1976) and Altiero and Gavazza (1980).

The availability of the closed form fundamental

solutions in two-dimensional anisotropic elasticity owes to the complex variable formalisms developed by Lekhnitskii (1963), Green and Zerna (1954), Milne-Thomson (1960) in plane stress and strain and to Eshelby *et al.* (1953), Stroh (1958; 1962), and Barnett and Lothe (1973) in generalized plane strain. The latter is the most general case of two-dimensional anisotropy in which the in-plane and the out-of-plane deformations are coupled. In Stroh's formalism the duality (Ni and Nemat-Nasser, 1996) exists between the displacement and the stress function fields which leads to a pair of fundamental solutions consisting of the dislocation and the point force. An important consequence of this duality, in the BEM formulation, is the physical interpretation of Somigliana's identity; the displacement in a finite body R subject to the displacement u_i and the traction t_i on the boundary ∂R can be given by the continuous distributions of dislocation dipoles and point forces of magnitudes u_i and t_i, respectively, along a closed contour ∂R embedded in an infinite body. One of the primary objectives of this paper is to adopt the Stroh's formalism and exploit the duality relations in the formulation of the BEM for the in-plane deformation of anisotropic solids that is uncoupled from the out-of-plane deformation. We will provide the explicit formulas for the displacement and the traction BEM formulations, obtained by analytical integration of the boundary integrals.

The main objective of the BEM for anisotropic cracked bodies is the calculation of the stress intensity factors. Tan and Gao (1992), with the quarter-point traction and displacement crack tip elements, used analytical expressions for the stress intensity factors given in terms of the nodal traction and displacement of these elements. Sollero and Aliabadi (1993), with the dual boundary element method, used the J-integral and the ratio of the crack opening displacements near the crack tip. Snyder and Cruse (1975) used the Green's function for a single crack in an infinite domain and obtained the stress intensity factors analytically without modeling the crack surface. For problems involving a crack or an elliptical or circular hole, the use of the Green's functions that satisfy the special boundary condition on the crack or the hole has been a popular approach in the BEM as seen in Clements and Haselgrove (1983), Kamel and Liaw (1989a, b; 1991) for plane stress and strain and Ang and Clements (1986), Berger and Tewary (1986), Hwu and Yen (1991), Hwu and Liao (1994), Tan *et al.* (1992) for generalized plane strain. Although the crack Green's function BEM gives accurate stress intensity factor results, it is limited to a single straight crack.

To demonstrate the capability of the BEM developed, we apply the method to mixed mode crack problems for multiply cracked anisotropic bodies. We extend the physical interpretation of Somigliana's identity to cracked bodies and represent the crack by the continuous distribution of dislocation dipoles. For the calculation of the stress intensity factors, we adopt the conservation integrals of elasticity developed by Chen and Shield (1977) and successfully implemented by Wang *et al.* (1980) in their FEM fracture analysis of cracked anisotropic bodies. It is known that the J-integral can be evaluated in a region away from the crack tip where the stress and deformation fields can be calculated more accurately than at the crack tip. It is however limited to the calculation of Mode I stress intensity factors. We demonstrate that the combination of the conservation integrals and the BEM developed here gives us a superb tool for the mixed mode crack analysis for multiple crack problems.

II. BASIC EQUATIONS IN PLANE ANISOTROPIC ELASTICITY

In this paper we consider the plane anisotropic elasticity problems where the displacement $\boldsymbol{u}$ depends only on two coordinates x_1 and x_2. We further assume that the anisotropic material possesses, at each point, a plane of symmetry normal to x_3-axis (i.e., out-of-plane axis) such that the in-plane and the out-of-plane deformations are decoupled. Only the in-plane problems (i.e., plane strain and generalized plane stress) described by the displacement components u_1 and u_2 are considered.

In describing the stress, strain, stiffness and compliance components it is convenient to replace a pair of suffices ij by a single suffix M according to the convention (11→1), (22→2), (33→3), (23→4), (31→5) (12→6). Note that the suffices 4 and 5 are absent in our in-plane problems. The non zero strain components (in engineering notation) are given by

$$e_1=u_{1,1},\ e_2=u_{2,2},\ e_6=u_{2,1}+u_{1,2}, \tag{1}$$

where a comma followed by a subscript i indicates the differentiation by x_i. The compatibility equation to be satisfied by the strain components is given, from (1), by

$$e_{2,11}+e_{1,22}-e_{6,12}=0. \tag{2}$$

In plane strain, where $\sigma_3=0$, the strain-stress relations are given by

$$e_M=s_{MN}\sigma_N \quad (M, N=1, 2, 6), \tag{3}$$

where s_{MN} are the elastic compliances and the summation over the repeated index is implied. In plane strain, where $e_3=0$, we get the reduced relations

$$e_M=S_{MN}\sigma_N \quad (M, N=1, 2, 6), \tag{4}$$

where the reduced compliances S_{MN} are given by

$$S_{MN}=s_{MN}-(s_{M3}s_{3N})/s_{33} \quad (M, N=1, 2, 6).$$

Introduce the stress vectors $\boldsymbol{\sigma}_1=\{\sigma_{11}, \sigma_{12}\}^T$ and $\boldsymbol{\sigma}_2=\{\sigma_{21}, \sigma_{22}\}^T$. The force equilibrium equation, with no body force, is given by

$$\frac{\partial \boldsymbol{\sigma}_1}{\partial x_1}+\frac{\partial \boldsymbol{\sigma}_2}{\partial x_2}=0. \tag{5}$$

Also introduce a real-valued stress function vector $\boldsymbol{\psi}=\{\psi_1, \psi_2\}^T$ such that

$$\boldsymbol{\sigma}_1=-\frac{\partial \boldsymbol{\psi}}{\partial x_2}, \quad \boldsymbol{\sigma}_2=\frac{\partial \boldsymbol{\psi}}{\partial x_1}, \tag{6}$$

then the equilibrium Eq. (5) is automatically satisfied.

According to Lekhnitskii (1963) and Eshelby *et al.* (1953) the solution of the plane problem can be represented by two analytic functions $f_1(z_1)$, $f_2(z_2)$ of the arguments $z_\alpha=x_1+p_\alpha x_2$, where p_α are two distinct complex numbers, which are roots of the fourth-order polynomial characteristic equations introduced later. The displacement u_i, stress σ_{ij} and the resultant force r_i along an arc are represented in the form

$$u_i=2\Re[\sum_{\alpha=1}^{2} A_{i\alpha}f_\alpha(z_\alpha)], \quad r_i=-2\Re[\sum_{\alpha}^{2} L_{i\alpha}f_\alpha(z_\alpha)]$$

$$\sigma_{2i}=2\Re[\sum_{\alpha=1}^{2} L_{i\alpha}f'_\alpha(z_\alpha)], \quad \sigma_{1i}=-2\Re[\sum_{\alpha=1}^{2} L_{i\alpha}p_\alpha f'_\alpha(z_\alpha)], \tag{7}$$

where $(\,)'$ indicates the derivative with respect to the argument of the function, and $A_{i\alpha}$ and $L_{i\alpha}$ are the components of two 2×2 matrices $\boldsymbol{A}$ and $\boldsymbol{L}$ to be defined below.

Assume the stress function vector

$$\boldsymbol{\phi}=\boldsymbol{l}f(x_1+px_2), \tag{8}$$

of the form where $\boldsymbol{l}=\{L_1, L_2\}^T$ and substitute it in the compatibility Eq. (2). In plane stress, this results in the fourth-order characteristic equation in p

$$s_{11}p^4-2s_{16}p^3+(2s_{12}+s_{66})p^2-2s_{26}p+s_{22}=0. \tag{9}$$

It is shown that the Eq. (9) has two pairs of conjugate complex roots p_1, $\overline{p_1}$, p_2, $\overline{p_2}$. Without loss of generality the imaginary part of p_α (α=1, 2) is assumed to be positive. In the following treatment we assume that the two roots p_1, p_2 are distinct. In the numerical analysis the degenerate case of coincident roots can be handled by slightly perturbing compliance coefficients to make them distinct. The elements of matrix $\boldsymbol{L}$, obtained from the compatibility equation, are given by

$$\boldsymbol{L}=[\boldsymbol{l}_1, \boldsymbol{l}_2]=\begin{bmatrix} -p_1L_{21} & -p_2L_{22} \\ L_{21} & L_{22} \end{bmatrix}. \tag{10}$$

The matrix $\boldsymbol{A}$, obtained by integrating the strain components, is given by

$$\boldsymbol{A}=[\boldsymbol{a}_1, \boldsymbol{a}_2], \tag{11}$$

with

$$\boldsymbol{a}_\alpha=\begin{Bmatrix} A_{1\alpha} \\ A_{2\alpha} \end{Bmatrix}=\begin{bmatrix} s_{16}-s_{11}p_\alpha & s_{12} \\ \dfrac{s_{26}-s_{21}p_\alpha}{p_\alpha}, & \dfrac{s_{22}}{p_\alpha} \end{bmatrix}\begin{Bmatrix} L_{1\alpha} \\ L_{2\alpha} \end{Bmatrix}. \tag{12}$$

The characteristic equation and the matrices $\boldsymbol{L}$ and $\boldsymbol{A}$ for plane strain are obtained by replacing the compliances s_{MN} with the reduced compliances S_{MN}.

Note that for each characteristic root p_α vectors $\boldsymbol{l}$ and $\boldsymbol{a}$ are determined to within an arbitrary multiplying factor. The typical normalization is given by

$$L_{21}=L_{22}=1 \tag{13}$$

in (10). Another normalization, based on the orthogonal relations (Stroh, 1958; 1962), is given by

$$2\sum_{i=1}^{2} L_{i\alpha}A_{i\alpha}=1 \quad (\text{no sum on } \alpha;\ \alpha=1, 2). \tag{14}$$

III. FUNDAMENTAL SOLUTIONS

Consider a point force and a dislocation of magnitudes $\boldsymbol{r}=\{F_1, F_2\}^T$ and $\boldsymbol{b}=\{b_1, b_2\}^T$, respectively located at $\xi=\eta_1+i\eta_2$ in the z-plane. The solution is given by the complex potential functions

$$f_\alpha(z_\alpha)=\frac{1}{2\pi i}(L_{j\alpha}b_j+A_{j\alpha}F_j)\ln(z_\alpha-\xi_\alpha)$$

$$(\text{no sum on } \alpha;\ \alpha=1, 2), \tag{15}$$

which, upon a circuit around ξ, give the force resultant $-\boldsymbol{r}$ and the displacement jump $\boldsymbol{b}$. Here, $\xi_\alpha=\eta_1+p_\alpha\eta_2$ and the elements of the matrices $\boldsymbol{L}$ and $\boldsymbol{A}$ are normalized by (14). Note that the summation over the repeated index j is implied.

The displacement, the displacement gradient and the stress contributions at z are given, from (7), in

index notation by

$$u_i(z)=2\Re\{\frac{1}{2\pi i}\sum_{\alpha=1}^{2}A_{i\alpha}(L_{j\alpha}b_j+A_{j\alpha}F_j)\ln(z_\alpha-\xi_\alpha)\}, \quad (16)$$

$$u_{i,1}(z)=2\Re\{\frac{1}{2\pi i}\sum_{\alpha=1}^{2}A_{i\alpha}(L_{j\alpha}b_j+A_{j\alpha}F_j)\frac{1}{z_\alpha-\xi_\alpha}\},$$

$$u_{i,2}(z)=2\Re\{\frac{1}{2\pi i}\sum_{\alpha=1}^{2}p_\alpha A_{i\alpha}(L_{j\alpha}b_j+A_{j\alpha}F_j)\frac{1}{z_\alpha-\xi_\alpha}\}, \quad (17)$$

$$\sigma_{1i}(z)=-2\Re\{\frac{1}{2\pi i}\sum_{\alpha=1}^{2}p_\alpha L_{i\alpha}(L_{j\alpha}b_j+A_{j\alpha}F_j)\frac{1}{z_\alpha-\xi_\alpha}\},$$

$$\sigma_{2i}(z)=2\Re\{\frac{1}{2\pi i}\sum_{\alpha=1}^{2}L_{i\alpha}(L_{j\alpha}b_j+A_{j\alpha}F_j)\frac{1}{z_\alpha-\xi_\alpha}\}. \quad (18)$$

Define a force dipole as a pair of plus and minus forces of the equal magnitude located at an infinitesimal distance apart. A dislocation dipole is defined similarly in terms of a pair of dislocations, which results in an infinitesimal line segment that has a displacement discontinuity. For the force and dislocation dipoles located at ξ, the displacement, its gradient and the stress contributions at z are given by

$$u_i^{(d)}(z)=2\Re\{\frac{1}{2\pi i}\sum_{\alpha=1}^{2}A_{i\alpha}(L_{j\alpha}b_j+A_{j\alpha}F_j)d\{\ln(z_\alpha-\xi_\alpha)\}, \quad (19)$$

$$u_{i,1}^{(d)}(z)=2\Re\{\frac{1}{2\pi i}\sum_{\alpha=1}^{2}A_{i\alpha}(L_{j\alpha}b_j+A_{j\alpha}F_j)d\{\frac{1}{z_\alpha-\xi_\alpha}\}\},$$

$$u_{i,2}^{(d)}(z)=2\Re\{\frac{1}{2\pi i}\sum_{\alpha=1}^{2}p_\alpha A_{i\alpha}(L_{j\alpha}b_j+A_{j\alpha}F_j)d\{\frac{1}{z_\alpha-\xi_\alpha}\}\}, \quad (20)$$

$$\sigma_{1i}^{(d)}(z)=-2\Re\{\frac{1}{2\pi i}\sum_{\alpha=1}^{2}p_\alpha L_{i\alpha}(L_{j\alpha}b_j+A_{j\alpha}F_j)d\{\frac{1}{z_\alpha-\xi_\alpha}\}\},$$

$$\sigma_{2i}^{(d)}(z)=2\Re\{\frac{1}{2\pi i}\sum_{\alpha=1}^{2}L_{i\alpha}(L_{j\alpha}b_j+A_{j\alpha}F_j)d\{\frac{1}{z_\alpha-\xi_\alpha}\}\}, \quad (21)$$

where

$$d\{\ln(z_\alpha-\xi_\alpha)\}=-\frac{d\xi_\alpha}{z_\alpha-\xi_\alpha}\ \text{(no sum on }\alpha),$$

$$d\{\frac{1}{z_\alpha-\xi_\alpha}\}=\frac{d\xi_\alpha}{(z_\alpha-\xi_\alpha)^2}\ \text{(no sum on }\alpha), \quad (22)$$

are the total derivatiives of $\ln(z_\alpha-\xi_\alpha)$ and $\frac{1}{z_\alpha-\xi_\alpha}$ with respect to ξ_α.

IV. DIRECT FORMULATION OF THE BEM IN 2-D

1. Physical Interpretation of Somigliana's Identity in Plane Anisotropic Elasticity

Consider a finite domain R with the boundary ∂R subject to the boundary displacement $\boldsymbol{u}=\{u_1, u_1\}^T$ and the traction $\boldsymbol{t}=\{t_1, t_2\}^T$. According to a physical interpretation of Somigliana's identity (Altiero and Gavazza, 1980; Eshelby, 1969; Denda and Dong, 1997; Denda and Kosaka, 1997) the displacement field in the domain R is given by the distributions of point forces and dislocations of magnitudes t_j and u_j, respectively, over the contour ∂R embedded in the infinite domain. To arrive at this physical interpretation, consider the following imaginary series of cutting, applying stress, scraping and welding operations. First, cut around the region R and remove it from infinite region leaving the outside region R^- behind. Then, apply the original set of loading to the region R resulting in the traction t_i and the displacement u_i on the boundary ∂R that give rise to the final displacement field in R. The outside region R^- is undeformed. To accommodate the deformed region R back in the hole, scrape away material from the surface of the hole where interpenetration is expected and fill in the material where gap occurs, put the deformed region R back in the hole and weld. A pair of boundary points, one in R and another in R^-, which were coincident before the set of operations are now separated, thus giving rise to a displacement discontinuity. The entire array of such discontinuities results in a layer of dislocation dipoles along the interface of the two regions. The applied traction has become built in as a layer of body forces along the interface. The final displacement field in the inside region is the same as that in the finite body R and zero in the outside region R^-.

Let Γ represent a boundary element. The displacement, the displacement gradient and the stress contributions of the continuous distribution of point forces with the magnitude $\boldsymbol{t}$ over Γ are given, from (16)-(18), by

$$u_i^t(z)=2\Re\{\frac{1}{2\pi i}\sum_{\alpha=1}^{2}\int_{\Gamma_\alpha}A_{i\alpha}A_{j\alpha}t_j(\xi_\alpha)\ln(z_\alpha-\xi_\alpha)ds\}, \quad (23)$$

$$u_{i,1}^t(z)=2\Re\{\frac{1}{2\pi i}\sum_{\alpha=1}^{2}\int_{\Gamma_\alpha}A_{i\alpha}A_{j\alpha}t_j(\xi_\alpha)\frac{1}{z_\alpha-\xi_\alpha}ds\},$$

$$u_{i,2}^t(z)=2\Re\{\frac{1}{2\pi i}\sum_{\alpha=1}^{2}\int_{\Gamma_\alpha}p_\alpha A_{i\alpha}A_{j\alpha}t_j(\xi_\alpha)\frac{1}{z_\alpha-\xi_\alpha}ds\}, \quad (24)$$

$$\sigma^t_{1i}(z) = -2\Re\{\frac{1}{2\pi i}\sum_{\alpha=1}^{2}\int_{\Gamma_\alpha} p_\alpha L_{i\alpha}A_{j\alpha}t_j(\xi_\alpha)\frac{1}{z_\alpha-\xi_\alpha}ds\},$$

$$\sigma^t_{2i}(z) = 2\Re\{\frac{1}{2\pi i}\sum_{\alpha=1}^{2}\int_{\Gamma_\alpha} L_{i\alpha}A_{j\alpha}t_j(\xi_\alpha)\frac{1}{z_\alpha-\xi_\alpha}ds\}, \quad (25)$$

where s is the arc length along the element Γ and Γ_α is the image of the element Γ in the induced plane z_α. The index i ranges from 1 to 2 and the summation for the repeated index j is taken from 1 to 2. The contributions of the continuous distribution of dislocation dipoles with the magnitude $\boldsymbol{u}$ over Γ are given, from (19)-(21), by

$$u^u_i(z) = 2\Re\{\frac{1}{2\pi i}\sum_{\alpha=1}^{2}\int_{\Gamma_\alpha} A_{i\alpha}L_{j\alpha}u_j(\xi_\alpha)d\{\ln(z_\alpha-\xi_\alpha)\},$$

(26)

$$u^u_{i,1}(z) = 2\Re\{\frac{1}{2\pi i}\sum_{\alpha=1}^{2}\int_{\Gamma_\alpha} A_{i\alpha}L_{j\alpha}u_j(\xi_\alpha)d\{\frac{1}{z_\alpha-\xi_\alpha}\}\},$$

$$u^u_{i,2}(z) = 2\Re\{\frac{1}{2\pi i}\sum_{\alpha=1}^{2}\int_{\Gamma_\alpha} p_\alpha A_{i\alpha}L_{j\alpha}u_j(\xi_\alpha)d\{\frac{1}{z_\alpha-\xi_\alpha}\}\},$$

(27)

$$\sigma^u_{1i}(z) = -2\Re\{\frac{1}{2\pi i}\sum_{\alpha=1}^{2}\int_{\Gamma_\alpha} p_\alpha L_{i\alpha}L_{j\alpha}u_j(\xi_\alpha)d\{\frac{1}{z_\alpha-\xi_\alpha}\}\},$$

$$\sigma^u_{2i}(z) = 2\Re\{\frac{1}{2\pi i}\sum_{\alpha=1}^{2}\int_{\Gamma_\alpha} L_{i\alpha}L_{j\alpha}u_j(\xi_\alpha)d\{\frac{1}{z_\alpha-\xi_\alpha}\}\}.$$

(28)

2. Interpolation

Let us consider a straight boundary element Γ with end points ξ_1 and ξ_2 and the slope ϕ. In each of the induced planes z_α (α=1, 2) Γ is mapped to another straight line Γ_α with end points $\xi_{\alpha1}$ and $\xi_{\alpha2}$. Let s be the arc length parameter of the element Γ in the physical plane z. For a straight element there exists one-to-one relation between the length s and the complex coordinate ξ of the element. Further, since each of the generalized complex variables ξ_α (α=1, 2) is uniquely related to ξ, we can express the density functions u_j and t_j (j=1, 2) in terms of ξ_α. In this paper we use the quadratic interpolation of the density functions given by

$$u_j(\xi_\alpha) = \sum_{n=1}^{3}\varphi_n(\xi_\alpha)u_{jn}, \quad t_j(\xi_\alpha) = \sum_{n=1}^{3}\varphi_n(\xi_\alpha)t_{jn}, \quad (29)$$

where $\psi_n(\xi_\alpha)$ (n=1, 2, 3) are the quadratic shape functions and u_{jn} and t_{jn} are the nodal values of the density functions u_j and t_j at node n. The quadratic interpolation requires three nodes: two end nodes at the end points ξ_1 and ξ_2 of the line Γ and a middle node at the mid-point ξ_3. The shape functions are given by

$$\varphi_n(\xi_\alpha) = \frac{(\xi_\alpha-\xi_{\alpha m})(\xi_\alpha-\xi_{\alpha o})}{(\xi_{\alpha n}-\xi_{\alpha m})(\xi_{\alpha n}-\xi_{\alpha o})}$$

(n=1, 2, 3 and $m\neq o\neq n$), (30)

where no summation is taken over the repeated indices. Let us denote the pth derivative, with respect to ξ_α, of the density functions by $u_j^{(p)}(\xi_\alpha)$ and $t_j^{(p)}(\xi_\alpha)$, then

$$u_j^{(p)}(\xi_\alpha) = \sum_{n=1}^{3}\varphi_n^{(p)}(\xi_\alpha)u_{jn}, \quad t_j^{(p)}(\xi_\alpha) = \sum_{n=1}^{3}\varphi_n^{(p)}(\xi_\alpha)t_{jn},$$

(p=0, 1, 2),

where $\varphi_\alpha^{(p)}(\xi_\alpha)$ indicates the pth derivative of the shape function with respect to ξ_α.

3. Displacement, Displacement Gradient and Stress

Since the function $\ln(z_\alpha-\xi_\alpha)$ is multi-valued it is necessary to define the unique value of this function by introducing a branch cut. Note that ξ_α is located on the line Γ_α and the line is directed positive from $\xi_{\alpha1}$ to $\xi_{\alpha2}$. The most convenient branch cut for $\ln(z_\alpha-\xi_\alpha)$ is defined by a straight line connecting ξ_α (the branch point) and $\xi_{\alpha1}$ (the first end point of Γ_α) and extending it to the infinity in the negative direction of Γ_α. Let θ_α^U ($-\pi<\theta_\alpha^U\leq+\pi$) be the principal value argument of $\ln(z_\alpha-\xi_\alpha)$ as z_α approaches Γ_α from the left. Then, we define the argument of $\ln(z_\alpha-\xi_\alpha)$ according to

$$\theta_\alpha^U - 2\pi < \arg(z_\alpha-\xi_\alpha) \leq \theta_\alpha^U. \quad (31)$$

Integrals in (23) and (26), with the interpolation (29), can be evaluated analytically for the straight element Γ giving the displacement contributions at z by

$$u^t_i(z) = \sum_{n=1}^{3}U^{(t)}_{ijn}(z)t_{jn},$$

$$u^u_i(z) = \sum_{n=1}^{3}U^{(u)}_{ijn}(z)u_{jn}, \quad (32)$$

with

$$U^{(t)}_{ijn}(z) = 2\Re\{\frac{1}{2\pi i}\sum_{\alpha=1}^{2}A_{i\alpha}A_{j\alpha}\mathcal{U}^{(t)}_{n\alpha}(z_\alpha)\},$$

$$U^{(t)}_{ijn}(z) = 2\Re\{\frac{1}{2\pi i}\sum_{\alpha=1}^{2}A_{i\alpha}A_{j\alpha}\mathcal{U}^{(u)}_{n\alpha}(z_\alpha)\}, \quad (33)$$

and

$$\mathcal{U}^{(t)}_{n\alpha}(z_\alpha)=\frac{1}{\cos\phi+p_\alpha\sin\phi}$$

$$\cdot\sum_{d=1}^{3}(-1)^{d-1}[\varphi_n^{(d-1)}(\xi_\alpha)\ln^{[d]}(z_\alpha-\xi_\alpha)]_{\xi\alpha1}^{\xi\alpha2},$$

$$\mathcal{U}^{(u)}_{n\alpha}(z_\alpha)=\sum_{d=0}^{2}(-1)^{d}[\varphi_n^{(d)}(\xi_\alpha)\ln^{[d]}(z_\alpha-\xi_\alpha)]_{\xi\alpha1}^{\xi\alpha2}, \tag{34}$$

where ϕ is the slope of the element Γ and $\ln^{[d]}(z_\alpha-\xi_\alpha)$ is the dth integral of $\ln(z_\alpha-\xi_\alpha)$ with respect to the argument ξ_α and is given by

$$\ln^{[d]}(z_\alpha-\xi_\alpha)=(-1)^d\frac{1}{d!}(z_\alpha-\xi_\alpha)^d\{\ln(z_\alpha-\xi_\alpha)-\sum_{j=1}^{d}\frac{1}{j}\}$$

$$(d\geq0). \tag{35}$$

When d is a negative integer $\ln^{[d]}(z_\alpha-\xi_\alpha)$ is interpreted as the derivative instead of the integral so that, for example,

$$\ln^{[-1]}(z_\alpha-\xi_\alpha)=-\frac{1}{z_\alpha-\xi_\alpha},\quad \ln^{[-2]}(z_\alpha-\xi_\alpha)=-\frac{1}{(z_\alpha-\xi_\alpha)^2},$$

Similarly, the displacement gradient contributions are obatined by integrating (24) and (27) analytically with the result

$$u^t_{i,k}(z)=\sum_{n=1}^{3}V^{(t)}_{ikjn}(z)t_{jn},$$

$$u^u_{i,k}(z)=\sum_{n=1}^{3}V^{(u)}_{ikjn}(z)u_{jn}, \tag{36}$$

where

$$V^{(t)}_{ikjn}(z)=2\Re\{\frac{1}{2\pi i}\sum_{\alpha=1}^{2}A_{i\alpha}A_{j\alpha}\mathcal{V}^{(t)}_{kn\alpha}(z_\alpha)\},$$

$$V^{(u)}_{ikjn}(z)=2\Re\{\frac{1}{2\pi i}\sum_{\alpha=1}^{2}A_{i\alpha}L_{j\alpha}\mathcal{V}^{(u)}_{kn\alpha}(z_\alpha)\}, \tag{37}$$

with

$$\mathcal{V}^{(t)}_{1n\alpha}(z_\alpha)=-\frac{1}{\cos\phi+p_\alpha\sin\phi}$$

$$\cdot\sum_{d=1}^{3}(-1)^{d-1}[\varphi_n^{(d-1)}(\xi_\alpha)\ln^{[d-1]}(z_\alpha-\xi_\alpha)]_{\xi\alpha1}^{\xi\alpha2},$$

$$\mathcal{V}^{(t)}_{2n\alpha}(z_\alpha)=p_\alpha\mathcal{V}^{(t)}_{1n\alpha}(z_\alpha),$$

$$\mathcal{V}^{(u)}_{1n\alpha}(z_\alpha)=-\sum_{d=0}^{2}(-1)^{d}[\varphi_n^{(d)}(\xi_\alpha)\ln^{[d-1]}(z_\alpha-\xi_\alpha)]_{\xi\alpha1}^{\xi\alpha2},$$

$$\mathcal{V}^{(u)}_{2n\alpha}(z_\alpha)=p_\alpha\mathcal{V}^{(t)}_{1n\alpha}(z_\alpha), \tag{38}$$

No summation is taken over the index α in (38).

The stress contributions are obtained by integrating (25) and (28) analytically with the result

$$\sigma^t_{ki}(z)=\sum_{n=1}^{3}S^{(t)}_{kijn}(z)t_{jn},$$

$$\sigma^u_{ki}(z)=\sum_{n=1}^{3}S^{(u)}_{kijn}(z)u_{jn}, \tag{39}$$

where

$$S^{(t)}_{kijn}(z)=2\Re\{\frac{1}{2\pi i}\sum_{\alpha=1}^{2}L_{i\alpha}A_{j\alpha}S^{(t)}_{kn\alpha}(z_\alpha)\},$$

$$S^{(u)}_{kijn}(z)=2\Re\{\frac{1}{2\pi i}\sum_{\alpha=1}^{2}L_{i\alpha}L_{j\alpha}S^{(u)}_{kn\alpha}(z_\alpha)\}, \tag{40}$$

with

$$S^{(t)}_{2n\alpha}(z_\alpha)=-\frac{1}{\cos\phi+p_\alpha\sin\phi}$$

$$\cdot\sum_{d=1}^{3}(-1)^{d-1}[\varphi_n^{(d-1)}(\xi_\alpha)\ln^{[d-1]}(z_\alpha-\xi_\alpha)]_{\xi\alpha1}^{\xi\alpha2},$$

$$S^{(t)}_{1n\alpha}(z_\alpha)=-p_\alpha S^{(t)}_{2n\alpha}(z_\alpha),$$

$$S^{(u)}_{2n\alpha}(z_\alpha)=-\sum_{d=0}^{2}(-1)^{d}[\varphi_n^{(d)}(\xi_\alpha)\ln^{[d-1]}(z_\alpha-\xi_\alpha)]_{\xi\alpha1}^{\xi\alpha2},$$

$$S^{(u)}_{1n\alpha}(z_\alpha)=-p_\alpha S^{(u)}_{2n\alpha}(z_\alpha). \tag{41}$$

No summation is taken over the index α in (41).

The traction $t_i=\nu_k\sigma_{ki}$ contributions on the segment with the unit normal ν_k are given from (39) by

$$t^t_i(z)=\sum_{n=1}^{3}T^{(t)}_{ijn}(z)t_{jn}=\sum_{n=1}^{3}\nu_kS^{(t)}_{kijn}(z)t_{jn},$$

$$t^u_i(z)=\sum_{n=1}^{3}T^{(u)}_{ijn}(z)u_{jn}=\sum_{n=1}^{3}\nu_kS^{(u)}_{kijn}(z)u_{jn}, \tag{42}$$

where $S^{(t)}_{kijn}(z)$ and $S^{(u)}_{kijn}(z)$ are given by (40) and (41). The summation is taken from 1 to 2 for the repeated indices j and k in (42).

4. Displacement and Traction Boundary Element Methods

In our formulation the boundary integrals are evaluated analytically and no distinction arises between the formulations of the interior and the exterior problems. Thus, we consider either a finite or infinite region R bounded by a closed contour ∂R which is subject to the traction t_i and the displacement u_i. The positive direction of the boundary ∂R is defined such that the material region is located to its left. We discretize and approximate the original boundary by a set of straight lines, $\partial\tilde{R}=\sum_{j=1}^{M}\Gamma_j$ where $\Gamma_j=\xi_j\xi_{j+1}$ (j=1, 2, ..., M) is the jth boundary element extending from node ξ_j to ξ_{j+1} with the slope ϕ_j.

In formulating the boundary element method following the physical interpretation of Somigliana's identity and the discretization mentioned above, we

can use the results obtained in Section IV.3.

(1) Displacement BEM

This formulation is based on the displacement contributions from the point force (t_i) and the dislocation dipole (u_i) distributions over an element given by (32)-(34). The displacement in the body is given by adding the two contributions, i.e.,

$$u_i = u_i^t + u_i^u ,$$

and the contributions from all the boundary elements to set up the field equation in the displacement BEM. In setting up the system of boundary equations, using the continuous boundary element, the terms $\ln^{[d]}(z_\alpha - \xi_\alpha)$ for d=1, 2 and 3 in (34) go to zero as z approaches the end nodes, while the term $\ln^{[0]}(z_\alpha - \xi_\alpha) = \ln|z_\alpha - \xi_\alpha| + i\arg(z_\alpha - \xi_\alpha)$ is unbounded since its real part becomes infinite. However, at a given end node where two elements meet, the unbounded real part from the current element is canceled by another unbounded real part from the adjacent element. So we need to deal only with the imaginary part of $\ln^{[0]}(z_\alpha - \xi_\alpha)$, which may differ between two adjacent elements due to different selections of the branch cut.

(2) Traction BEM

This formulation uses the traction contributions (42) of the point force and the dislocation dipole distributions. The traction in the body is given by adding these two contributions,

$$t_i = t_i^t + t_i^u ,$$

and the contributions from all the boundary elements to set up the field Eq. As seen from (40)-(42) the traction becomes unbounded at the end nodes of the element. So we use the discontinuous boundary element for which the end collocation points, ξ_1^* and ξ_2^*, are shifted from the end points, ξ_1 and ξ_2, of the element. For the discontinuous boundary element the quadratic interpolation is still given by (29)-(30) if we substitute $\xi_{\alpha 1}^*$ and $\xi_{\alpha 2}^*$ for $\xi_{\alpha 1}$ and $\xi_{\alpha 2}$, respectively. In addition u_{jn} and t_{jn} (n=1, 2, 3) are the values of the density functions at ξ_1^*, ξ_2^*, and ξ_3. Other than the difference in the collocation scheme, the resulting expressions for the analytical integration are exactly the same for the continuous and the discontinuous boundary element schemes. The discontinuous boundary elements are used exclusively in the traction boundary element method even at nodes where the slope and the traction are continuous. A mixed use of the continuous and the discontinuous boundary elements in the displacement boundary element method is also possible.

V. MIXED MODE CRACK ANALYSIS

1. Mixed Displacement and Traction BEM for Crack Problems

Consider a crack in an infinite body introduced along a directed contour C with the upper and the lower surfaces C^+ and C^-, respectively. It is subject to the tractions T^+ and T^- and the displacements U^+ and U^- on the two surfaces. Apply the physical interpretation of Somigliana's identity to a flat elliptical hole which is subsequently collapsed into a crack along C. This procedure results in layers along C of point forces and dislocation dipoles with the densities $T_{cr}=T^+ + T^-$ and $\delta U = U^+ - U^-$, respectively. Here we consider the problem for which T^+ and T^- are specified on the entire crack surfaces and $T_{cr}=T^+ + T^- = 0$.

When the crack is treated as a single contour the displacement boundary element method cannot handle the problem (Cruse, 1989) while the traction boundary element method can. In setting up the traction boundary element method for the crack defined above the only boundary is the contour C on which the continuous distribution of the dislocation dipoles with density $\delta U = U^+ - U^-$ is placed. When T^+ and T^- are specified on the entire crack surfaces the only unknown is the crack opening displacement $\delta U = U^+ - U^-$. The system of boundary equations is obtained by equating the limiting values of the traction on the upper (or lower) crack surface to T^+ (or T^-) at boundary element nodes. Evaluation on only one side of the crack surfaces is sufficient to determine the unknown crack opening displacement.

When the crack is located in a finite body, including the crack intersecting its boundary, the effects of the non-crack boundary can be represented by the layers of point forces and dislocation dipoles as in the case of problems without the crack. Either the displacement or the traction boundary element method can be used for the non-crack boundary. The latter, in combination with the traction boundary element method for the crack, establishes the traction formulation and the former a mixed formulation (i.e., the traction and the displacement formulations for the crack and non-crack boundaries, respectively) for the crack problems. The mixed boundary element method is preferred since it allows the use of both the continuous and the discontinuous boundary elements on the non-crack boundary.

2. Conservation Law of Anisotropic Elasticity

Conservation laws in elasticity have been used effectively in the determination of the mixed mode

stress intensity factors for anisotropic materials both in the FEM and the BEM. Wang *et al.* (1980) have used a path independent integral, which is based on conservation laws of anisotropic elasticity defined for two equilibrium states (Chen and Shield, 1977, Wu, 1989). Chu and Hong (1990) used J_k (k=1, 2) integrals to determine stress intensity factors K_I and K_{II} using the FEM. Sollero and Aliabadi (1993) developed a BEM procedure based on J_1 integral and the ratio of relative crack opening displacements near the crack tip. We adopt the technique developed by Wang *et al.* (1980).

Introduce a local coordinate system O'–$x_1'x_2'$ at a tip O' of a crack such that x_1'-axis is tangent to the crack tip with the slope ϕ measured from the global x_1-axis. The crack need not be straight. In this coordinate system the J-integral is defined as

$$J' = \int_{\Gamma'} (W'n_1' - n_i'\sigma_{ij}'\frac{\partial u_j'}{\partial x_1'})ds', \tag{43}$$

where i, j=1, 2, Γ' is a contour surrounding the crack tip as shown in Fig. 1(a), W' is the strain energy density, σ_{ij}' and u_j' are the stress and the displacement, and n_i' is the unit normal to the path Γ'. Notice that in the local coordinate system the characteristic Eq. (9) is written in terms of the local compliance coefficients s_{MN}' in plane stress and local reduced compliance coefficients S_{MN}' in plane strain. We denote the local characteristic roots by p_1', $\bar{p}_1'$, p_2', $\bar{p}_2'$, which differ from those defined in the global coordinate system. Using expression for the energy release rate in mixed Mode I and II (Sih *et al.*, 1965), we can relate J' to the stress intensity factors by

$$J' = \alpha_{11}'K_I'^2 + \alpha_{12}'K_I'K_{II}' + \alpha_{22}'K_{II}'^2, \tag{44}$$

where

$$\alpha_{11}' = -\frac{s_{22}'}{2}\Im(\frac{p_1'+p_2'}{p_1'p_2'}),$$

$$\alpha_{22}' = \frac{s_{11}'}{2}\Im(p_1'+p_2'),$$

$$\alpha_{12}' = -\frac{s_{22}'}{2}\Im(\frac{1}{p_1'p_2'}) + \frac{s_{11}'}{2}\Im(p_1'p_2'), \tag{45}$$

in plane stress, where $\Im$ indicates the imaginary part. The results for plane strain are obtained by replacing s_{MN}' with S_{MN}'.

Note that (44) is not sufficient for the determination of K_I' and K_{II}'. Following Wang *et al.* (1980) consider two independent equilibrium states, 1° and 2°, in the local coordinate system with the displacements $u_i'^{(1)}$ and $u_i'^{(2)}$ and the stresses $\sigma_{ij}'^{(1)}$ and $\sigma_{ij}'^{(2)}$. The J-integral for the superposed state 0° is given

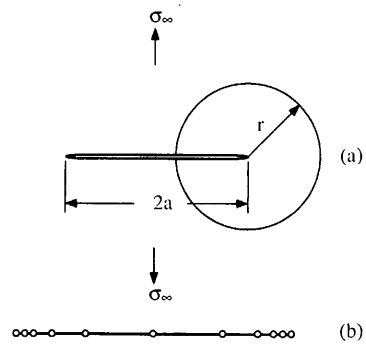

Fig. 1. (a) A center crack in an infinite body with a circular integration contour. (b) The mesh used for the crack.

(Chen and Shield, 1977) by

$$J'^{(0)} = J'^{(1)} + J'^{(2)} + M'^{(1,2)}, \tag{46}$$

where $J'^{(0)}$, $J'^{(1)}$ and $J'^{(2)}$ are local J-integrals for states 0°, 1° and 2° and $M'^{(1,2)}$ is defined by

$$M'^{(1,2)} = \int_{\Gamma'} [W'^{(1,2)}n_i' - (n_i'\sigma_{ij}'^{(1)}\frac{\partial u_j'^{(2)}}{\partial x_1'} + n_i'\sigma_{ij}'^{(2)}\frac{\partial u_j'^{(1)}}{\partial x_1'})]ds', \tag{47}$$

in terms of the mutual potential energy $W'^{(1,2)}$ defined by

$$W'^{(1,2)} = c_{ijkl}'\frac{\partial u_i'^{(1)}}{\partial x_j'}\frac{\partial u_k'^{(2)}}{\partial x_l'} = c_{ijkl}'\frac{\partial u_i'^{(2)}}{\partial x_j'}\frac{\partial u_k'^{(1)}}{\partial x_l'},$$

where c_{ijkl}' (with i, j, k, l=1, 2) are stiffness coefficients. The integral defined by (47) vanishes if the region surrounded by the integration contour does not contain any singularities (conservation law by Chen and Shield, 1977) and it is path independent for contours containing a crack tip. If we use the J–K relationship in (44) for states 0°, 1° and 2°, then we get

$$J'^{(0)} = J'^{(1)} + J'^{(2)} + 2\alpha_{11}'K_I'^{(1)}K_I'^{(2)} + \alpha_{12}'[K_I'^{(1)}K_{II}'^{(2)} + K_I'^{(2)}K_{II}'^{(1)}] + 2\alpha_{22}'K_{II}'^{(1)}K_{II}'^{(2)}. \tag{48}$$

Comparison of (46) and (48) gives

$$M'^{(1,2)} = 2\alpha_{11}'K_I'^{(1)}K_I'^{(2)} + \alpha_{12}'[K_I'^{(1)}K_{II}'^{(2)} + K_I'^{(2)}K_{II}'^{(1)}] + 2\alpha_{22}'K_{II}'^{(1)}K_{II}'^{(2)}. \tag{49}$$

Let the state 1° be the equilibrium state for the problem sought. Introduce the first known auxiliary solution, denoted by the superscript $2a$, given by the Mode I crack tip asymptotic solution in the local coordinate system with the stress intensity factor

$$K_I'^{2a} = 1 \text{ and } K_{II}'^{2a} = 0.$$

Table 1a. Engineering constants for laminates.

	E_1 ($\times 10^6$ psi)	E_2 ($\times 10^6$ psi)	G_{12} ($\times 10^6$ psi)	ν_{12}
$(0/\pm 45/90)_s$	8.7069	8.7069	3.4581	0.25829
$(0)_s$	21.000	1.7000	1.4000	0.21000
$(\pm 30)_s$	9.7161	2.5582	4.4871	0.99543
$(\pm 45)_s$	4.5223	4.5223	5.5162	0.61509
$(\pm 60)_s$	2.5582	9.7161	4.4871	0.26209
$(90)_s$	1.7000	21.000	1.4000	0.017000
$(90_2/\pm 45)_s$	4.0784	12.875	3.4581	0.17047
$(90_4/\pm 45)_s$	3.3805	15.634	2.7721	0.10503

Table 1b. Compliance constants for laminates ($\times 10^{-7}$ in^2/lb)

	s_{11}	s_{22}	s_{12}	s_{66}
$(0/\pm 45/90)_s$	0.28713	0.28713	-0.07434	0.72294
$(0)_s$	0.47619	5.8824	-0.10000	7.1429
$(\pm 30)_s$	0.51461	1.9545	-0.51226	1.1143
$(\pm 45)_s$	1.1056	1.1056	-0.68007	0.90642
$(\pm 60)_s$	1.9545	0.51461	-0.51226	1.1143
$(90)_s$	5.8824	0.47619	-0.10000	7.1429
$(90_2/\pm 45)_s$	0.61229	0.19418	-0.10450	0.72294
$(90_4/\pm 45)_s$	0.49303	0.10660	-0.051782	0.60124

In this case (49) is given by

$$M'^{(1,2a)} = 2\alpha'_{11}K'^{(1)}_I + \alpha'_{12}K'^{(1)}_{II} \tag{50}$$

and the integral $M'^{(1,2a)}$ has the form

$$M'^{(1,2a)} = \int_{\Gamma'} [c'_{ijkl}\frac{\partial u'^{(1)}_i}{\partial x'_j}\frac{\partial u'^{(2a)}_k}{\partial x'_l}n'_1 - (n'_i\sigma'^{(1)}_{ij}\frac{\partial u'^{(2a)}_j}{\partial x'_1} + n'_i\sigma'^{(2a)}_{ij}\frac{\partial u'^{(1)}_j}{\partial x'_1})]ds' . \tag{51}$$

Introduce the second auxiliary solution, denoted by the superscript $2b$, for Mode II asymptotic solution with the stress intensity factor

$$K'^{2b}_I = 0 \text{ and } K'^{2b}_{II} = 1 .$$

Equation (49) is given by

$$M'^{(1,2b)} = \alpha'_{12}K'^{(1)}_I + 2\alpha'_{22}K'^{(1)}_{II} \tag{52}$$

and the integral $M'^{(1,2b)}$ has the form

$$M'^{(1,2b)} = \int_{\Gamma'} [c'_{ijkl}\frac{\partial u'^{(1)}_i}{\partial x'_j}\frac{\partial u'^{(2b)}_k}{\partial x'_l}n'_1 - (n'_i\sigma'^{(1)}_{ij}\frac{\partial u'^{(2b)}_j}{\partial x'_1} + n'_i\sigma'^{(2b)}_{ij}\frac{\partial u'^{(1)}_j}{\partial x'_1})]ds' . \tag{53}$$

The auxiliary solutions $\sigma'^{(2a)}_{ij}$ and $u'^{(2a)}_i$ for Mode I and $\sigma'^{(2b)}_{ij}$ and $u'^{(2b)}_i$ for Mode II crack tip asymptotic solutions in the local coordinate system are given in terms of the local characteristic roots p'_1, $\bar{p}'_1$, p'_2, $\bar{p}'_2$ and are found in (Sih *et al.*, 1965) and (Wang *et al.*, 1980).

Equations (50)-(53) provide a system of linear Eqs. for $K'^{(1)}_I$ and $K'^{(1)}_{II}$. To evaluate the integrals $M'^{(1,2a)}$ and $M'^{(1,2b)}$ accurately we exploit the path independence and select a contour sufficiently away from the crack tip, where greater numerical accuracy can be achieved than near crack tip. In addition, we use the analytical BEM formulas of the stress and the displacement gradient solution, (39) and (36), for state 1° in its global coordinate system, from which the local solutions $\sigma'^{(1)}_{ij}$ and $u'^{(1)}_{i,j}$ are obtained by the coordinate transformation.

VI. NUMERICAL RESULTS

We have obtained numerical results for eight representative laminates: $(0)_s$, $(\pm 30)_s$, $(\pm 45)_s$, $(\pm 60)_s$, $(90)_s$, $(0/\pm 45/90)_s$, $(90_2/\pm 45)_s$, $(90_4/\pm 45)_s$. The engineering constants for the lamina are E_1=21×10^6 psi, E_2=1.7×10^6 psi, G_{12}=1.4×10^6 psi, ν_{12}=0.21, which are typical for a fiber-reinforced graphite epoxy (Snyder and Cruse, 1975). The engineering constants and the compliances for the eight laminates are listed in Table 1a and 1b, respectively.

Accuracy of the method is investigated by studying a center crack of length $2a$ in an infinite

Table 2. The effect of the integration contour on the stress intensity factor of a center crack in an infinite plate under uniaxial tension, where r is the radius of the circular contour and K_I^{anal} is the analytical solution.

r/a	K_I/K_I^{anal}	Rel. Error (%)	r/a	K_I/K_I^{anal}	Rel. Error (%)
0.005	0.87511	12.49	1.995	1.0075	0.75
0.05	1.0069	0.69	1.95	0.99149	0.85
0.1	0.99909	0.09	1.9	1.0000	0.00
0.2	0.99979	0.02	1.8	1.0011	0.11
0.3	0.99959	0.04	1.7	1.0003	0.03
0.4	1.0003	0.03	1.6	0.99965	0.03
0.5	0.99942	0.06	1.5	1.0003	0.03
0.6	1.0000	0.00	1.4	0.99983	0.02
0.7	1.0006	0.06	1.3	0.99943	0.06
0.8	1.0006	0.06	1.2	0.99942	0.06
0.9	1.0002	0.02	1.1	0.99974	0.03
1.0	0.99997	0.00			

quasi-isotropic laminate $(0/\pm45/90)_s$ subject to the uniaxial tension as shown in Fig. 1(a). In this paper the infinite plate is approximated by a finite but sufficiently large plate in comparison to the crack length $2a$. Fig. 1(b) shows the boundary element mesh for the crack with ten elements with the crack tip element size $1/16a$; this is the mesh used for all center cracks in this paper. For the calculation of the integrals $M'^{(1,\,2a)}$ and $M'^{(1,\,2b)}$ we have used circular integration paths (Fig. 1(a)) centered at each crack tip, divided the path into 18 equal intervals and adopted three point Gaussian quadrature formula for each interval. Finer intervals or more Gaussian points than used here had negligible improvement in the numerical accuracy. Table 2 shows the K_I values obtained for several circular paths with the radius r ranging from $r=0.005a$ (near crack tip) to $r=1.995a$ (near opposite crack tip). The path independence of the integrals can be seen over a wide range of contours. In the range between $r=0.1a$ and $r=1.9a$ the maximum relative error in K_I is 0.11%. The values of K_I for all eight laminates have clearly indicated its independence on the elastic constants, as shown by Sih *et al.* (1965) for a single crack in an infinite body. The remarkable accuracy, of the order between 0.1% and 1.0% either in the relative error with respect to the exact solution or in the deviation from the reliable reference values in literature, will be shown to hold not only for simple but also for more complex crack configurations as demonstrated below.

Figure 2 shows two collinear cracks in an infinite body subject to the uniaxial tension when $f=0$. The K_I values at crack tips A (inner) and B (outer) are listed in Table 3 for the quasi isotropic laminate $(0/\pm45/90)_s$. They are compared with values, for the isotropic materials, from the stress intensity handbook (Murakami *et al.*, 1987 with 0.5% accuracy) and those

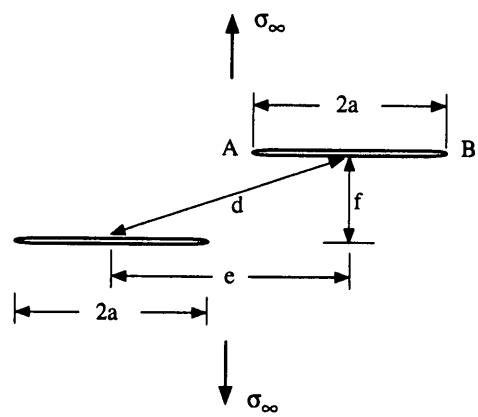

Fig. 2. Two parallel cracks in an infinite body under uniaxial tension: collinear if $f=0$ and aligned if $e=0$.

calculated by the whole crack singular element (Denda and Dong, 1997). Notice that the present results are slightly more accurate than those by Denda and Dong (1997) who incorporated the crack tip singularity analytically. This is a surprising but encouraging outcome, since the results by Denda and Dong (1997) have demonstrated the order of accuracy with less than 1% error. Fig. 3 shows three collinear cracks in an infinite body under tension. The K_I values for quasi isotropic laminate $(0/\pm45/90)_s$ are shown in Table 4 in comparison to values for the isotropic materials from the handbook (Murakami *et al.*, 1987). The typical deviation from the handbook value is 0.1%. For two and three collinear cracks, we have numerically verified that the K_I values are independent on the elastic constants. Sih *et al.* (1965) has proved such independence for a single crack in an infinite body with zero resultant force on the crack, but not for multiple collinear cracks. In order to demonstrate the dependence on the elastic constants, we

Table 3. Stress intensity factors for two collinear cracks in an infinite body.

$2a/d$	$K_{IB}/\sigma\sqrt{\pi a}$			$K_{IA}/\sigma\sqrt{\pi a}$		
	$(0/\pm45/90)_s$	Ref. [27]	Ref. [12]	$(0/\pm45/90)_s$	Ref. [27]	Ref. [12]
0.05	1.00036	1.00031	1.0018	1.00038	1.00032	1.0018
0.1	1.00127	1.00120	1.0027	1.00140	1.00132	1.0028
0.2	1.00470	1.00462	1.0061	1.00573	1.00566	1.0071
0.3	1.01023	1.01017	1.0117	1.01388	1.01383	1.0153
0.4	1.01791	1.01787	1.0194	1.02718	1.02717	1.0287
0.5	1.02796	1.02795	1.0295	1.04791	1.04796	1.0495
0.6	1.04090	1.04094	1.0426	1.07963	1.08040	1.0821
0.7	1.05776	1.05786	1.0596	1.13327	1.13326	1.1351
0.8	1.08084	1.08107	1.0827	1.22666	1.22894	1.2314
0.9	1.11687	1.11741	1.1187	1.44951	1.45387	1.4639

Table 4. Stress intensity factors for three collinear cracks in an infinite body, where $F_{IA}=K_{IA}/\sigma\sqrt{\pi a}$, $F_{IB}=K_{IB}/\sigma\sqrt{\pi a}$, $F_{IC}=K_{IC}/\sigma\sqrt{\pi a}$,

$2a/d$	F_{IA}		F_{IB}		F_{IC}	
	$(0/\pm45/90)_s$	Ref. [27]	$(0/\pm45/90)_s$	Ref. [27]	$(0/\pm45/90)_s$	Ref. [27]
0.05	1.00024	1.00083	1.00026	1.00040	1.00049	1.00063
0.1	1.00136	1.00150	1.00150	1.00164	1.00237	1.00252
0.2	1.00569	1.00585	1.00686	1.00702	1.01013	1.01030
0.3	1.01278	1.01296	1.01691	1.01710	1.02386	1.02407
0.4	1.02276	1.02297	1.03328	1.03353	1.04501	1.04529
0.5	1.03605	1.03631	1.05880	1.05913	1.07624	1.07663
0.6	1.05350	1.05383	1.09912	1.09915	1.12303	1.12316
0.7	1.07679	1.07724	1.16390	1.16456	1.19480	1.19558
0.8	1.10996	1.11032	1.28050	1.28348	1.31819	1.32126
0.9	1.16319	1.16439	1.55867	1.56454	1.60073	1.60685

have studied the problem of two parallel cracks arranged at various relative positions, from collinear through non-aligned to aligned, as shown in Fig. 2. The K_I values shown in Table 5 show their dependence on the elastic constants except for the collinear cracks with $e/f=\infty$. Comparison with results (Denda and Dong, 1997, (Murakami *et al.*, 1987) for isotropic materials, when available, shows deviation less than 0.5%.

Stress intensity factors for two aligned parallel cracks (Fig. 2 with $e=0$), three aligned parallel cracks (Fig. 4), and two inclined cracks (Fig. 5) are given in Tables 6, 7 and 8, respectively. Results, for the isotropic materials, from the handbook (Murakami *et al.*, 1987) and by Denda and Dong (1997) are also listed for comparison. For the two parallel cracks, the accuracy of the handbook values (Murakami *et al.*, 1987) is 5% for the case $2a/d=0.2$, 0.4, 0.8; that for $2a/d=1.0$, 2.0, 5.0 is unspecified. The deviation of our numerical results from the handbook values is less than 0.03% in $F_I=K_I/\sigma\sqrt{\pi a}$. For the three parallel cracks, the handbook values have the accuracy of 2% and our results for F_{IA} deviate from them less than

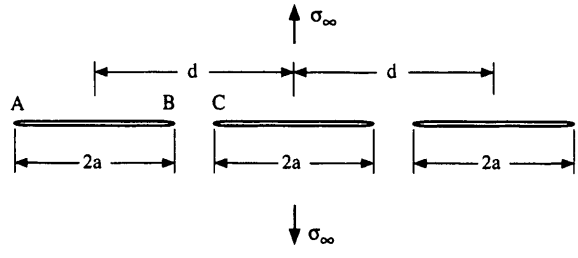

Fig. 3. Three collinear cracks in an infinite body under uniaxial tension.

0.1%. For the two inclined cracks less than 1% deviation in F_{IA} and F_{IB} is observed from the results by Denda and Dong (1997); numerical handbook values are not available.

A double-edge-cracked plate in tension is shown in Fig. 6, taken from Snyder and Cruse (1975), where the Green's function BEM that satisfies the crack face boundary condition automatically is used. The results are considered to be one of the most accurate for single crack problems. (Snyder and Cruse have analyzed one, instead of two, edge crack using the

Table 5. Dependence on the elastic constants of the stress intensity factors for two parallel cracks (collinear, non-aligned and algned) in an infinite body under tension, where $F_{IA}=K_{IA}/\sigma\sqrt{\pi a}$, $F_{IB}=K_{IB}/\sigma\sqrt{\pi a}$.

$d=2.5a$	e/f=0	e/f=0.5		e/f=1.0		e/f=2.0		e/f=inf	
	F_{IA}	F_{IA}	F_{IB}	F_{IA}	F_{IB}	F_{IA}	F_{IB}	F_{IA}	F_{IB}
Ref. [27]	0.8727							1.2289	1.0811
Ref. [12]	0.8732			0.94208		1.13712		1.2314	1.0827
$(0/\pm45/90)_s$	0.87237	0.84942	0.98539	0.94098	1.06039	1.13450	1.10222	1.22634	1.08056
$(0)_s$	0.92253	0.90872	0.96968	0.93901	1.01270	1.03623	1.06076	1.22641	1.08065
$(\pm30)_s$	0.95302	0.94360	0.94871	0.92759	0.98499	0.98781	1.07042	1.22631	1.08057
$(\pm45)_s$	0.93068	0.92237	0.93470	0.90565	1.02557	1.04412	1.10269	1.22639	1.08061
$(\pm60)_s$	0.85707	0.84430	0.99198	0.93601	1.09115	1.18042	1.12138	1.22631	1.08052
$(90)_s$	0.78877	0.69879	1.09374	1.05964	1.15122	1.33709	1.12339	1.22705	1.08116
$(90_2/\pm45)_s$	0.84103	0.80939	1.01403	0.96210	1.09563	1.20885	1.11696	1.22637	1.68056
$(90_4/\pm45)_s$	0.82257	0.77603	1.03883	0.98818	1.11268	1.25307	1.11956	1.22638	1.08056

Table 6. Aligned two parallel cracks in an infinite body under tension, where $F_I=K_I/\sigma\sqrt{\pi a}$.

	F_I					
	$2a/d$=0.2	0.4	0.8	1.0	2.0	5.0
Ref. [27]	0.9855	0.9508	0.8727	0.8319	0.7569	0.6962
Ref. [12]	0.987	0.9517	0.8732	0.844	0.7746	0.7129
$(0/\pm45/90)_s$	0.9857	0.9505	0.8724	0.8433	0.7733	0.7228
$(0)_s$	0.9929	0.9741	0.9225	0.8979	0.8183	0.7505
$(\pm30)_s$	0.9971	0.9885	0.9530	0.9278	0.8192	0.7383
$(\pm45)_s$	0.9968	0.9862	0.9307	0.8916	0.7862	0.7188
$(\pm60)_s$	0.9890	0.9553	0.8571	0.8232	0.7547	0.7068
$(90)_s$	0.9357	0.8580	0.7888	0.7723	0.7344	0.7075
$(90_2/\pm45)_s$	0.9792	0.9309	0.8410	0.8140	0.7547	0.7120
$(90_4/\pm45)_s$	0.9696	0.9095	0.8226	0.7994	0.7477	0.7103

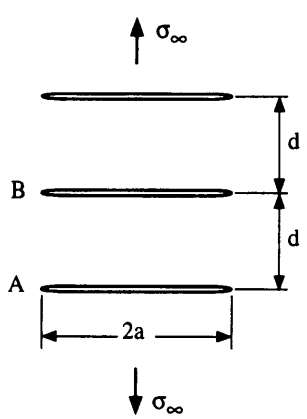

Fig. 4. Three aligned parallel cracks in an infinite body under uniaxial tension.

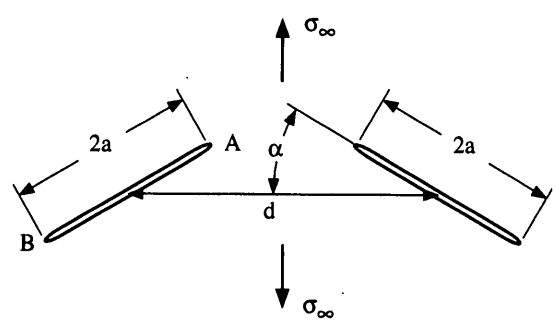

Fig. 5. Two inclined cracks in an infinite body under uniaxial tension.

symmetry condition.) We have adopted the mesh used by Snyder and Cruse (Fig. 8 in (Snyder and Cruse, 1975)) consisting of 50 elements for the whole boundary. The results are shown in Table 9 in comparison with those by Snyder and Cruse (1975). The maximum deviation from the results by Snyder and Cruse (1975) is 0.76%. Although the present method is capable of dealing with multiple curvilinear cracks in finite bodies, numerical results for comparison are not available in literature except for the current example of a double-edge-cracked plate.

The last two problems are concerned with a semi-infinite body subject to the uniaxial tension. Fig. 7(a) shows a kinked crack in a semi-infinite body in tension. The meshes used for the non-crack

Table 7. Aligned two parallel cracks in an infinite body under tension, where $F_{IA}=K_{IA}/\sigma\sqrt{\pi a}$.

	F_{IA}							
	$2a/d$=0.1	0.2	0.3	0.4	0.5	0.6	0.7	0.8
Ref. [27]	0.99500	0.98198	0.96299	0.9401	0.91535	0.8908	0.86851	0.85052
$(0/\pm45/90)_s$	0.9953	0.9822	0.9628	0.9396	0.9151	0.8913	0.8692	0.8494
$(0)_s$	0.9977	0.9911	0.9809	0.9679	0.9530	0.9373	0.9213	0.9056
$(\pm30)_s$	0.9990	0.9964	0.9920	0.9858	0.9779	0.9682	0.9569	0.9442
$(\pm45)_s$	0.9990	0.9961	0.9910	0.9833	0.9726	0.9585	0.9414	0.9218
$(\pm60)_s$	0.9965	0.9865	0.9697	0.9469	0.9197	0.8912	0.8642	0.8407
$(90)_s$	0.9750	0.9212	0.8697	0.8302	0.8015	0.7804	0.7645	0.7521
$(90_2/\pm45)_s$	0.9931	0.9743	0.9473	0.9167	0.8865	0.8592	0.8358	0.8164
$(90_4/\pm45)_s$	0.9896	0.9626	0.9272	0.8913	0.8593	0.8327	0.8113	0.7941

Table 8. Two inclined cracks in an infinite body under tension, where $F_{IA}=K_{IA}/\sigma\sqrt{\pi a}$, $F_{IB}=K_{IB}/\sigma\sqrt{\pi a}$, $F_{IIA}=K_{IIA}/\sigma\sqrt{\pi a}$, $F_{IIB}=K_{IIB}/\sigma\sqrt{\pi a}$.

	α=30°					
	$2a/d$=0.1		$2a/d$=0.5		$2a/d$=0.9	
	F_{IA}	F_{IB}	F_{IA}	F_{IB}	F_{IA}	F_{IB}
Ref. [12]	0.7503	0.7503	0.7718	0.7595	0.914	0.7881
$(0/\pm45/90)_s$	0.7504	0.7503	0.7715	0.7594	0.9111	0.7878
$(0)_s$	0.7500	0.7495	0.7870	0.7408	0.9993	0.7527
$(\pm30)_s$	0.7502	0.7501	0.7678	0.7538	0.9228	0.7707
$(\pm45)_s$	0.7504	0.7503	0.7697	0.7596	0.8998	0.7871
$(\pm60)_s$	0.7505	0.7505	0.7721	0.7625	0.8996	0.7963
$(90)_s$	0.7502	0.7502	0.7731	0.7635	0.9011	0.8005
$(90_2/\pm45)_s$	0.7505	0.7504	0.7722	0.7622	0.9023	0.7955
$(90_4/\pm45)_s$	0.7505	0.7505	0.7726	0.7627	0.9021	0.7974

	α=30°					
	$2a/d$=0.1		$2a/d$=0.5		$2a/d$=0.9	
	F_{IIA}	F_{IIB}	F_{IIA}	F_{IIB}	F_{IIA}	F_{IIB}
$(0/\pm45/90)_s$	0.4332	0.4332	0.4373	0.4426	0.4535	0.4745
$(0)_s$	0.4324	0.4332	0.3918	0.4613	0.2964	0.5261
$(\pm30)_s$	0.4330	0.4331	0.4287	0.4426	0.3901	0.4828
$(\pm45)_s$	0.4332	0.4332	0.4389	0.4413	0.4575	0.4702
$(\pm60)_s$	0.4333	0.4333	0.4430	0.4417	0.4881	0.4678
$(90)_s$	0.4331	0.4331	0.4445	0.4417	0.5015	0.4671
$(90_2/\pm45)_s$	0.4333	0.4333	0.4422	0.4419	0.4838	0.469
$(90_4/\pm45)_s$	0.4333	0.4333	0.4431	0.4419	0.4901	0.4684

boundary and for the crack are shown in Fig. 7(b) and Fig. 7(c), respectively. The non-crack boundary and the crack consist of 34 and 12 (6 for each of the straight crack segment) nonhomogeneous elements, respectively. Fig. 8(a) shows two parallel edge cracks in a semi-infinite body in tension. The meshes for the non-crack boundary (with 26 elements) and for the cracks (6 elements for each crack) are shown in Fig. 8(b) and Fig. 8(c), respectively. Numerical results for the stress intensity factors for the two problems are given in Tables 10 and 11. Results for isotropic materials by the handbook (Murakami *et al.*, 1987) and by Denda and Dong (1999), where singular crack tip element is used, are also listed. The current results for F_I deviate from the handbook values by less than 0.5% for both crack configurations.

VII. CONCLUDING REMARKS

We have used Stroh complex variable formalism and the physical interpretation of Somigliana's identity to develop a boundary element method for

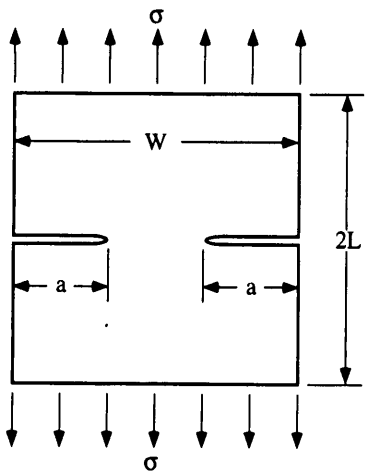

Fig. 6. Double edge cracks in a plate in tension.

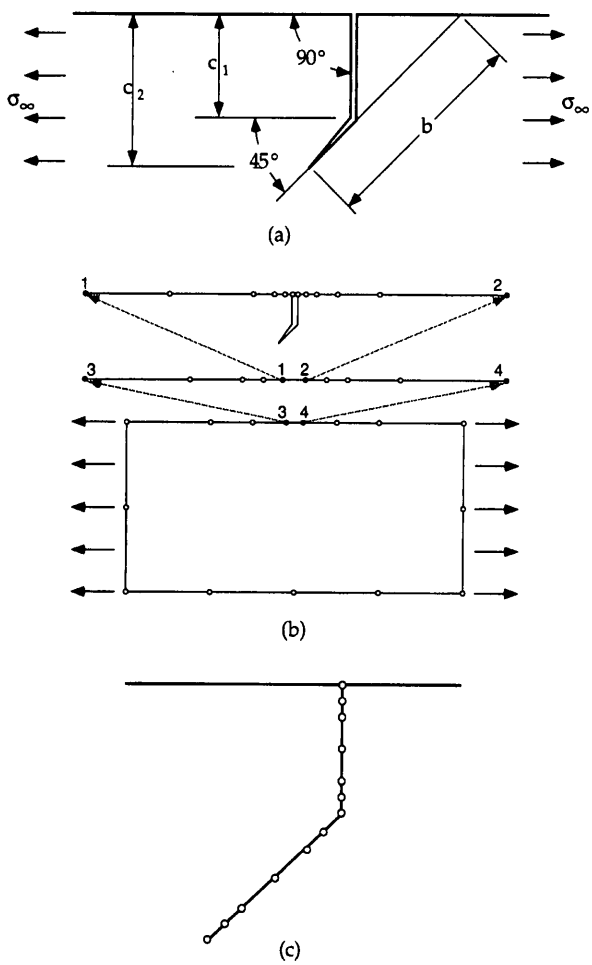

Fig. 7. (a) A kinked crack in a semi-infinite plate in tension; (b) mesh for non-crack boundary and (c) crack elements for the kinked crack.

Table 9. Double-edge-cracked plate in tension.

	$K_I/\sigma\sqrt{a}$	
	Present	Ref. [31]
$(0)_s$	1.977	1.962
$(\pm30)_s$	2.099	2.095
$(\pm45)_s$	2.154	2.159
$(\pm60)_s$	2.102	2.107
$(90)_s$	2.021	2.008
$(0/\pm45/90)_s$	2.010	2.023
$(90_2/\pm45)_s$	2.025	2.023
$(90_4/\pm45)_s$	2.008	2.004

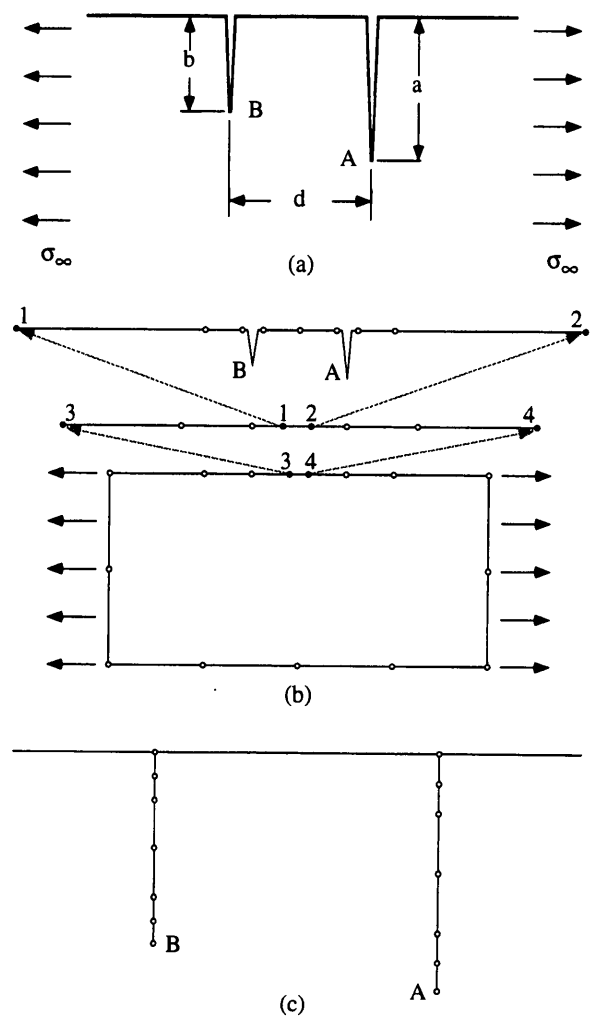

Fig. 8. (a) Two parallel edge cracks in a semi-infinite plate in tension; (b) mesh for non-crack boundary and (c) crack elements.

plane anisotropic elasticity problems involving multiple cracks. We have developed simple boundary element method formulas through analytical integration of the boundary integrals. These formulas have been applied to the mixed mode crack analysis for multiple cracks with the help of the conservation integrals. They are concise yet the stress

Table 10. A kinked crack in a semi-infinite plate in tension, where c_2=1.0 in Fig. 7(a) and $F_I=K_I/\sigma\sqrt{\pi b}$, $F_{II}=K_{II}/\sigma\sqrt{\pi b}$.

	c_1=0.25		c_1=0.5		c_1=0.75		c_1=0.9	
	F_I	F_{II}	F_I	F_{II}	F_I	F_{II}	F_I	F_{II}
Ref. [27]	0.703	-0.365	0.704	-0.365	0.705	-0.366	0.707	-0.359
Ref. [13]	0.706	-0.365	0.706	-0.365	0.706	-0.366	0.706	-0.359
$(0/\pm45/90)_s$	0.7040	-0.3666	0.7042	-0.3667	0.7032	-0.3674	0.7047	-0.3595
$(0)_s$	0.9137	-0.1245	0.8899	-0.1487	0.9047	-0.1328	0.9135	-0.1275
$(\pm30)_s$	0.8809	-0.2039	0.8856	-0.2005	0.8815	-0.2081	0.8823	-0.1991
$(\pm45)_s$	0.7747	-0.3473	0.7775	-0.3450	0.7797	-0.3448	0.7815	-0.3361
$(\pm60)_s$	0.6776	-0.4549	0.6776	-0.4544	0.6777	-0.4527	0.6784	-0.4458
$(90)_s$	0.5897	-0.4875	0.5897	-0.4875	0.5896	-0.4865	0.5900	-0.4821
$(90_2/\pm45)_s$	0.6540	-0.4400	0.6542	-0.4397	0.6541	-0.4387	0.6549	-0.4320
$(90_4/\pm45)_s$	0.6308	-0.4576	0.6310	-0.5903	0.6308	-0.4565	0.6315	-0.4505

Table 11. Two parallel edge cracks in a semi-infinite plate in tension, where $d=a$ and $F_{IA}=K_{IA}/\sigma\sqrt{\pi b}$, $F_{IB}=K_{IB}/\sigma\sqrt{\pi b}$.

	b/a=0.25		b/a=0.5		b/a=0.75		b/a=0.9	
	F_{IA}	F_{IB}	F_{IA}	F_{IB}	F_{IA}	F_{IB}	F_{IA}	F_{IB}
Ref. [27]	1.118	0.214	1.094	0.418	1.015	0.644	0.854	0.854
Ref. [13]	1.124	0.208	1.1	0.413	1.021	0.643	0.858	0.858
$(0/\pm45/90)_s$	1.1218	0.2119	1.0976	0.4157	1.0194	0.6455	0.8584	0.8584
$(0)_s$	1.0852	0.5425	1.0509	0.6393	0.9824	0.7585	0.8738	0.8738
$(\pm30)_s$	1.1589	0.5804	1.1178	0.6855	1.0432	0.8126	0.9330	0.9330
$(\pm45)_s$	1.2024	0.3072	1.1637	0.5400	1.0753	0.7643	0.9361	0.9361
$(\pm60)_s$	1.1832	0.0449	1.1638	0.3184	1.0746	0.6292	0.8881	0.8881
$(90)_s$	1.0971	-0.0226	1.0933	0.1289	1.0502	0.3838	0.8026	0.8025
$(90_2/\pm45)_s$	1.1359	0.067	1.1206	0.2933	1.0440	0.5748	0.8508	0.8508
$(90_4/\pm45)_s$	1.1224	0.031	1.1118	0.236	1.0439	0.5186	0.8337	0.8337

intensity factor results obtained by them are accurate to within 1% of the values provided by the handbook (Murakami *et al.*, 1987) and other reliable sources (Denda and Dong, 1987; Denda and Dong, 1999).

Although the BEM developed here can be readily extended to generalized plane strain for which the in-plane and out-of-plane deformations are coupled, its application to the mixed mode crack analysis requires the development of formulas for the energy release rate and the conservation integrals. This is not a trivial task and requires a separate paper.

REFERENCES

1. Altiero, N.J., and Gavazza, S.D., 1980, "On a Unified Boundary-integral Equation Method," *Journal of Elasticity*, Vol. 10, No. 1, pp. 1-9.
2. Ang, W.T., and Clements, D.L., 1986, "A Boundary Element Method for Determining the Effect of Holes on the Stress Distribution around a Crack," *International Journal for Numerical Methods Engineering*, Vol. 23, pp. 1727-1737.
3. Balas, J., Sladek, J., and Sladek, V., 1989, *Stress Analysis by Boundary Element Methods*, Elsevier, Amsterdam.
4. Barnett, D.M., and Lothe, J., 1973, "Synthesis of the Sextic and the Integral Formalism for Dislocation, Green's Functions and Surface Waves in Anisotropic Elastic Solids," *Physica Norvegica* Vol. 7, pp. 13-19.
5. Benjumea, R., and Sikarskie, D.C., 1972, "On the Solution of Plane Orthotropic Elasticity Problems by an Integral Equation Method," *Journal of Applied Mechanics*, Vol. 39, pp. 801-808.
6. Berger, J.R., and Tewary, V.K., 1986, "Boundary Integral Equation Formulation for Interface Cracks in Anisotropic Materials," *International Journal for Numerical Methods in Engineering*, Vol. 23, pp. 1727-1737.
7. Chen, F.H.K., and Shield, R.T., 1977, "Conservation Laws in Elasticity of the J-Integral Type," *Journal of Applied Mathematics and Physics (ZAMP)*, Vol. 28, pp. 1-22.
8. Chu, S.J., and Hong, C.S., 1990, "Application of

the J_k Integral to Mixed Mode Crack Problems for Anisotropic Composite Laminates," *Engineering Fracture Mechanics*, Vol. 35, pp. 1093-1103.
9. Clements, D.L., and Haselgrove, M.A., 1983, "A Boundary Integral Equation for a Class of Crack Problems in Anisotropic Elasticity," *International Journal of Computer Mathematics*, Vol. 12, pp. 267-278.
10. Crouch, S.L., and Starfield, A.M., 1983, *Boundary Element Methods in Solid Mechanics, George Allen and Unwin Publishers*, London.
11. Cruse, T.A., 1989, *Boundary Element Analysis in Computational Fracture Mechanics*, Kluwer Academic Publishers, Dordrecht.
12. Denda, M., and Dong, Y.F., 1997, "Complex Variable Approach to the BEM for Multiple Crack Problems," *Computer Methods Applied Mechanics Engineering*, Vol. 141, pp. 247-264.
13. Denda, M., and Dong, Y.F., 1999, "Analytical Formulas for a 2-D Crack-Tip Singular Boundary Element for Curvilinear Cracks and Crack Growth Analysis," *International Journal of Engineering Analysis with Boundary Elements*, Vol. 23, No. 1, pp. 35-49.
14. Denda, M., and Kosaka, I., 1997, "Dislocation and Point-Force-Based Approach to the Special Green's Function BEM for Elliptic Hole and Crack Problems in Two Dimensions," *International Journal for Numerical Methods in Engineering*, Vol. 40, pp. 2857-2889.
15. Eshelby, J.D., 1969, "The Elastic Field of a Crack Extending Non-Uniformly under General Anti-Plane Loading," *Journal of Mechanics Physics of Solids*, Vol. 17, pp. 177-199.
16. Eshelby, J.D., Read W.T., and Shockley, W., 1953, "Anisotropic Elasticity with Applications to Dislocation Theory," *Acta Metall*urgica, Vol. 1, pp. 251-259.
17. Green, A.E., and Zerna, W., 1954, *Theoretical Elasticity*, Oxford at the Clarendon Press, Oxford.
18. Hwu, C., and Liao, C.Y., 1994, "A Special Boundary Element for the Problems of Multi-Holes, Cracks and Inclusions," *Computers and Structures*, Vol. 51, No. 1, pp. 23-31.
19. Hwu, C., and Yen, W.J., 1991, "Green's Functions of Two-Dimensional Anisotropic Plates Containing and Elliptic Hole," *International Journal of Solids and Structures*, Vol. 27, No. 13, pp. 1705-1719.
20. Kamel, M., and Liaw, B.M., 1989a, "Analysis of a Loaded Elliptical Hole or a Crack in an Anisotropic Plate," *Mechanics Research Communication*, Vol. 16, No. 6, pp. 379-383.
21. Kamel, M., and Liaw, B.M., 1989b, "Green's Functions due to Concentrated Moments Applied in an Anisotropic Plate with an Elliptic Hole or a Crack," *Mechanics Research Communication*, Vol. 16, No. 5, pp. 311-319.
22. Kamel, M., and Liaw, B.M., 1991, "Boundary Element Formulation with Special Kernels for an Anisotropic Plate Containing an Elliptical Hole or a Crack," *Engineering Fracture Mechanics*, Vol. 39, No. 4, pp. 695-711.
23. Lee, K.L., and Mal, A.K., 1990, "A Boundary Element Method for Plane Anisotropic Elastic Media," *Journal of Applied Mechanics*, Vol. 57, pp. 600-606.
24. Lekhnitskii, S.G., 1963, *Theory of Elasticity of an Anisotropic Elastic Body*, Hoden-Day, San Francisco.
25. Maiti, M., Das, B., and Palit, S.S., 1976, "Somigliana's Method Applied to Plane Problems of Elastic Half-Spaces," *Journal of Elasticity*, Vol. 6, pp. 429-439.
26. Milne-Thomson, L.M., 1960, *Plane Elastic Systems, Springer-Verlag*, Berlin.
27. Murakami *et al.*, Y., 1987, *Stress Intensity Factor Handbook*, Pergamon Press, Oxford.
28. Ni, L., and Nemat-Nusser, S., 1996, "General Duality Principle in Elasticity," *Mechanics of Materials*, Vol. 24, No. 2, pp. 87-123.
29. Rizzo, F.J., and Shippy, D.J., 1970, "A Method for Stress Determination in Plane Anisotropic Bodies," *Journal of Composite Materials*, Vol. 4, pp. 36-61.
30. Sih, G.C., Paris, P.C., and Irwin, G.R., 1965, "On Cracks in Rectilinearly Anisotropic Bodies," *International Journal of Fracture*, Vol. 1, No. 3, pp. 189-203.
31. Snyder, M.D., and Cruse, T.A., 1975, "Boundary Integral Equation Analysis of Cracked Anisotropic Plates," *International Journal of Fracture*, Vol. 11, pp. 315-328.
32. Sollero, P., and Aliabadi, M.H., 1993, "Fracture Mechanics Analysis of Anisotropic Plates by the Boundary Element Method," *International Journal of Fracture*, Vol. 64, No. 4, pp. 269-284.
33. Stroh, A.N., 1958, "Dislocations and Cracks in Anisotropic Elasticity," *Philosophical Mag*azine, Vol. 7, pp. 625-646.
34. Stroh, A.N., 1962, "Steady State Problems in Anisotropic Elasticity," *Journal of Mathematics and Physics*, Vol. 41, pp. 77-103.
35. Tan, C.I., and Gao, Y.L., 1992, "Boundary Element Analysis of Plane Anisotropic Bodies with Stress Concentrations and Cracks," *Composite Structures*, Vol. 20, pp. 17-28.
36. Tan, C.L., Gao, Y.L., and Afagh, F.F., 1992, "Boundary Element Analysis of Interface Cracks Between Dissimilar Anisotropic Materials," *International Journal of Solids Strucutres*, Vol. 29, No. 24, pp. 3201-3220.

37. Wang, S.S., Yau, J.F., and Corten, H.T., 1980, "A Mixed-Mode Crack Analysis of Rectilinear Anisotropic solids using Conservation Laws of Elasticity," *International Journal of Fracture*, Vol. 16, No. 3, pp. 247-259.
38. Wu, K.C., 1989, "Representation of Stress Intensity Factors by Path-independent Integrals," *Journal of Applied Mechanics*, Vol. 56, pp. 780-785.

Discussions of this paper may appear in the discussion section of a future issue. All discussions should be submitted to the Editor-in-Chief.

Manuscript Received: Apr. 09, 1999
Revision Received: May 30, 1999
and Accepted: July 12, 1999

以差排與點作用力之模式的邊界元素法進行異向性的平面混合模式裂縫分析

M. Denda

美國紐澤西州羅格斯大學機械學與航太工程學系

摘 要

本文推導平面異向性彈力問題的邊界元素法（即：將面內變形與面外變形分開討論），基於差排偶極與點作用力的分佈，根據Somigliana掇恆等式的物理解釋，在一個有限體 R 的位移場可表示爲沿著埋藏於有限域中的虛邊界（R）來分配選擇差排偶極與點作用力，我們採用異向性彈性的 Stroh 複數形式，來代表差排與點作用力，及其偶極，與有系統地利用差排解與點作用力的對偶性關係之連續分佈。利用公式可得到位移和曳引力（位移的法向微分）在邊界積分方程的解析解，應用這些公式可針對在多連通裂縫異向體中之混合模式的裂縫問題，以Somigliana恆等式來擴展物理的解釋與表示裂縫的差排偶極之連續分佈，藉著異向性彈性的積分值守恆，以驗證其可行性，並正確地決定此混合模式的應力強度因子（K_I and K_{II}）。

關鍵字：邊界元素法，平面的異向性彈性問題，差排與點作用力的分佈法，混合模式的裂縫分析。